University of Nebraska - Lincoln

DigitalCommons@University of Nebraska - Lincoln

February 2001

Heterogeneity within Animal Thioredoxin Reductases

Qi-An Sun
University of Nebraska-Lincoln

Francesca Zappacosta
SmithKline Beecham Pharmaceuticals, King of Prussia, Pennsylvania

Valentina M. Factor
NCI, National Institutes of Health, Bethesda, Maryland

Peter J. Wirth
NCI, National Institutes of Health, Bethesda, Maryland

Dolph L. Hatfield
NCI, National Institutes of Health, Bethesda, Maryland

See next page for additional authors

Authors

Qi-An Sun, Francesca Zappacosta, Valentina M. Factor, Peter J. Wirth, Dolph L. Hatfield, and Vadim N. Gladyshev

Heterogeneity within Animal Thioredoxin Reductases

EVIDENCE FOR ALTERNATIVE FIRST EXON SPLICING*

Qi-An Sun‡, Francesca Zappacosta§, Valentina M. Factor¶, Peter J. Wirth¶, Dolph L. Hatfield‖, and Vadim N. Gladyshev‡

From the ‡Department of Biochemistry, University of Nebraska, Lincoln, Nebraska 68588, the §SmithKline Beecham Pharmaceuticals, King of Prussia, Pennsylvania 19406, the ¶Laboratory of Experimental Carcinogenesis, NCI, National Institutes of Health, Bethesda, Maryland 20892, and the ‖Basic Research Laboratory, NCI, National Institutes of Health, Bethesda, Maryland 20892

Animal thioredoxin reductases (TRs) are selenocysteine-containing flavoenzymes that utilize NADPH for reduction of thioredoxins and other protein and nonprotein substrates. Three types of mammalian TRs are known, with TR1 being a cytosolic enzyme, and TR3, a mitochondrial enzyme. Previously characterized TR1 and TR3 occurred as homodimers of 55–57-kDa subunits. We report here that TR1 isolated from mouse liver, mouse liver tumor, and a human T-cell line exhibited extensive heterogeneity as detected by electrophoretic, immunoblot, and mass spectrometry analyses. In particular, a 67-kDa band of TR1 was detected. Furthermore, a novel form of mouse TR1 cDNA encoding a 67-kDa selenoprotein subunit with an additional N-terminal sequence was identified. Subsequent homology analyses revealed three distinct isoforms of mouse and rat TR1 mRNA. These forms differed in 5′ sequences that resulted from the alternative use of the first three exons but had common downstream sequences. Similarly, expression of multiple mRNA forms was observed for human TR3 and *Drosophila* TR. In these genes, alternative first exon splicing resulted in the formation of predicted mitochondrial and cytosolic proteins. In addition, a human TR3 gene overlapped with the gene for catechol-*O*-methyltransferase (COMT) on a complementary DNA strand, such that mitochondrial TR3 and membrane-bound COMT mRNAs had common first exon sequences; however, transcription start sites for predicted cytosolic TR3 and soluble COMT forms were separated by ~30 kilobases. Thus, this study demonstrates a remarkable heterogeneity within TRs, which, at least in part, results from evolutionary conserved genetic mechanisms employing alternative first exon splicing. Multiple transcription start sites within TR genes may be relevant to complex regulation of expression and/or organelle- and cell type-specific location of animal thioredoxin reductases.

The thioredoxin redox system is one of two major redox systems in animal cells, which, together with the glutathione system, participates in the redox control of a great variety of biological processes involved in cell life and death (1–3). Disruption of the gene for thioredoxin 1, a 12-kDa thiol disulfide oxidoreductase, results in embryonic lethality in mice (4) demonstrating an essential role of the thioredoxin system in the development of mammals. Three distinct thioredoxin reductases (TRs)[1] (5–10) are responsible for maintaining thioredoxins in a reduced state and are also capable of reducing a great variety of other protein and nonprotein redox substrates. The cytosolic thioredoxin reductase (TR1), the most characterized of the three enzymes, was known for decades, but only recently it was found to be a selenium-containing protein (11). TR1 contains a C-terminal penultimate selenocysteine residue encoded by TGA (12), and this residue is essential for catalytic activity of the enzyme (13–15).

One of the first indications that multiple TR forms occur in mammalian cells was immunoblot analyses of various human TR preparations. An enzyme possessing TR activity that was isolated from a human lung adenocarcinoma cell line NCI-H441 failed to react with antibodies specific for rat liver TR1 (11), whereas TR isolated from a human T-cell line JPX9 reacted with these antibodies (12). Determination of internal peptide sequences of the T-cell TR demonstrated that this protein was TR1 (12). Unfortunately, the NCI-H441 enzyme was not sequenced, and in retrospect it seems possible, that this TR could have been encoded by a different gene. In addition to a TR form not reacting with anti-TR1 antibodies, subsequent studies identified two forms of TR1 isolated from either NCI-H441 or HeLa cells that showed a positive immunoblot signal with these antibodies (16–18). Yet, these forms differed in catalytic activity, selenium content, and affinity for column matrices. In particular, forms that differed in the ability to bind to a heparin column were extensively characterized (16–18). However, differences in either protein or gene sequences, or in post-translational modifications that were responsible for the observed changes in catalytic and chromatographic properties, were not reported.

Recently, two additional thioredoxin reductases, TR2 and TR3, were identified that contained the conserved selenocysteine residue (5–10). These enzymes had also other sequences essential for catalytic activity, including an N-terminal disulfide active center, NADPH- and FAD-binding domains and dimer interface sequences (5–10). The three TR enzymes

[1] The abbreviations used are: TR, thioredoxin reductase; TGFα, transforming growth factor α; PAGE, polyacrylamide gel electrophoresis; HPLC, high performance liquid chromatography; MALDI, matrix-assisted laser desorption ionization; GPx, glutathione peroxidase; Sec, selenocysteine; NR, nonredundant; COMT, catechol-*O*-methyltransferase; MB-COMT, membrane-bound catechol-*O*-methyltransferase; S-COMT, soluble catechol-*O*-methyltransferase; AD, Alzheimer's disease.

showed >50% sequence identity, although TR1 and TR2 were closely related enzymes, while TR3 was a more evolutionary distant enzyme (10). TR3 (also called TRβ (5) and TrxR2 (6)), like TR1, appeared to be ubiquitously expressed (5–10). This enzyme was described as a mitochondrial thioredoxin reductase because it was shown to contain a mitochondrial signal peptide. In addition, this protein was localized in mitochondria by detecting various transiently expressed, tagged forms of TR3 and by immunoblot assays with antibodies specific for TR3 (5–10). TR2 had not been extensively characterized nor its full amino acid sequence reported (10).

In the present report, we describe the occurrence of multiple forms of TR1 and TR3 and utilize genetic and biochemical techniques to characterize the basis for heterogeneity within animal TR preparations. We find differences in 5′-end cDNA sequences for mammalian TR1, mammalian TR3, and *Drosophila* TR that resulted from the alternative use of first exons.

EXPERIMENTAL PROCEDURES

Partial Isolation of Mouse TRs from Normal Livers and Liver Tumors on an ADP-Sepharose Column—Male wild type and transforming growth factor α (TGFα)/c-*myc* double transgenic mice (6–15 months old) were maintained and labeled with ^{75}Se, and their livers and liver tumors were dissected as described previously (19). The coexpression of TGFα and c-Myc results in multiple liver tumor formation by 6 months of age. Three unlabeled wild type mouse livers (4 g) and a single ^{75}Se-labeled wild type liver (0.5 g) were mixed and homogenized in 10 ml of 40 mM Tris-HCl, pH 7.5, 100 mM NaCl, 1 mM EDTA, 0.6 mM 4-(2-aminoethyl)benzenesulfonyl fluoride, 5 μg/ml aprotinin, and 5 μg/ml leupeptin (buffer A). The homogenate was centrifuged at 18,000 rpm for 20 min, and the supernatant was loaded directly onto a 3-ml ADP-Sepharose (Amersham Pharmacia Biotech) column. The column was washed extensively with 150 mM NaCl and 40 mM Tris-HCl, pH 7.5, and proteins were eluted with 1 M NaCl in 40 mM Tris-HCl, pH 7.5. Protein fractions were tested by SDS-PAGE and immunoblot analyses with antibodies specific for TR1 and TR3 (10), pooled, and further analyzed by a two-dimensional gel electrophoresis. TR1 was also isolated from TGFα/c-*myc* tumors using the same procedure except that 5 unlabeled liver tumors (11.5 g) and one ^{75}Se-labeled liver tumor (3.5 g) were homogenized in 15 ml of buffer A.

TR1 Purification—TR1 was isolated from mouse liver, rat prostate, and a human T-cell line JPX9 according to a three-step procedure that involved DEAE-Sepharose (Amersham Pharmacia Biotech), ADP-Sepharose, and phenyl-HPLC columns (TosoHaas) as described previously (12). To obtain ^{75}Se-labeled TR1, unlabeled mouse livers were mixed with a single ^{75}Se-labeled wild type liver. Isolated proteins were analyzed by immunoblot assays with antibodies specific for TR1, TR2, and TR3 (10), protein staining with Coomassie Blue and by detecting ^{75}Se with a PhosphorImager (Molecular Dynamics). To further fractionate the enzyme, TR1 preparation was dialyzed against 20 mM Tris-HCl, pH 7.0, and applied onto a heparin-HPLC column (TosoHaas). The proteins were eluted with a gradient of 20–500 mM Tris-HCl, pH 7.0. ^{75}Se was detected in fractions with a γ-counter. JPX9 cells were grown on an RPMI 1640 medium in the presence of 10% fetal bovine serum and metabolically labeled with ^{75}Se as described previously (12). Human A431 cell line was grown as described (10) and TRs were purified from sonicated crude extracts on an ADP-Sepharose column as described for mouse enzymes.

Two-dimensional Gel Electrophoresis—Two-dimensional gel electrophoresis of ^{75}Se-contining polypeptides was performed as described previously (20). Briefly, 25 μl of each TR preparation (500 μg of total protein), which was partially purified on an ADP-Sepharose column, were resolved in the first dimension on an isoelectric focusing (IEF) gel, followed by separation in the second dimension on a 10% polyacrylamide gel under reducing conditions. The separated polypeptides were electroblotted on polyvinylidene difluoride membranes, the blots stained with Ponceau S, and the ^{75}Se-containing proteins detected on the dried membranes by the PhosphorImager analysis.

Peptide Mapping—TR samples purified by one-dimensional or two-dimensional gel electrophoresis were transferred onto polyvinylidene difluoride membranes and stained with either Ponceau S or Sulforodamine B. Bands were excised and digested with trypsin as described (21). After digestion, peptides were extracted from the membrane with the addition of 10 μl of formic acid:ethanol (1:1) for 1 h at room temperature. 0.5 μl were sampled directly from the supernatant to the matrix-assisted laser desorption ionization (MALDI) plate, mixed with 0.5 μl of α-cyano-4-hydroxy cinnamic acid matrix (10 mg/ml in acetonitrile/trifluoroacetic acid, 0.1%) and allowed to air-dry before data collection. Spectra were acquired on a Voyager RP mass spectrometer using oxidized bovine insulin β chain as internal standard for calibration (21, 22).

Mass Spectrometric Analysis of Intact Human TR Molecules—Mass spectrometric analysis of native or alkylated human TR proteins was performed on a API300 triple quadrupole mass spectrometer equipped with a Micro-IonSpray source. Prior to MS analysis proteins were purified by RP-HPLC on a narrow-bore Vydac C4 column (150 × 2.1 mm, 5 μm) using a linear gradient of 0–70% acetonitrile containing 0.1% trifluoroacetic acid and a flow rate of 250 μl/min. Samples were manually collected and directly injected into the mass spectrometer ion source by infusion at 1 μl/min. Reduction and alkylation of TRs was conducted in denaturing conditions (6 M guanidine HCl, pH 8.0) using iodoacetamide as an alkylating agent.

Other Procedures—Mouse cDNA clones (clone ID 607552, accession number AI662374, Stratagene mouse skin cDNA library; and clone ID 2064717, accession number AI789478, Sugano mouse kidney-mkia cDNA library) were purchased from Research Genetics and their insert sequences experimentally determined. The two clones overlapped for 510 nucleotides and the combined cDNA sequence was 3626 nucleotides long. SDS-PAGE, immunoblot, and isoelectrofocusing analyses were performed with electrophoretic supplies and gels from Novex. Immunoblot membranes were developed with a SuperSignal detection kit (Pierce) or an ECL detection kit (Amersham Pharmacia Biotech) using previously developed antibodies specific for TR1, TR2, and TR3 (10). We have previously demonstrated strict isozyme specificity of these antibodies (10). Nucleotide sequences were analyzed with BLAST programs (23). Exons were predicted with a NetGene2 program. Mitochondrial signal peptides were predicted with the PSORT II or SignalP programs.

RESULTS

Heterogeneity within Mouse Thioredoxin Reductase Preparations—To determine whether mouse TR1 occurs in multiple forms and if the distribution of these forms differs between normal and malignant cells, we partially isolated TRs from a pool of ^{75}Se-labeled wild type mouse livers and from a pool of ^{75}Se-labeled liver tumors developed in TGFα/c-*myc* double transgenic mice. To minimize potential losses of certain TR forms due to different elution profiles of these forms on columns commonly used in TR isolation procedures, we utilized only a single step, an affinity ADP-Sepharose chromatography, to purify TRs.

When ^{75}Se-labeled protein extracts obtained from either normal livers or liver tumors were fractionated on an ADP-Sepharose column, TR1, seen as a ^{75}Se-labeled band (Fig. 1*A, lanes 3* and *6*), and TR3, which is masked by TR1 due to its lower abundance (6, 10), were separated from the remainder of ^{75}Se-labeled proteins (Fig. 1*A*). Two other major ^{75}Se-labeled proteins that did not bind to the column were glutathione peroxidase 1 (GPx1) and glutathione peroxidase 4 (GPx4) (19). Since we used identical procedures for fractionation of normal and tumor samples, comparison of GPx1 and other selenoprotein bands in normal (Fig. 1*A, lane 1*) and tumor (Fig. 1*A, lane 4*) samples suggested that the levels of GPx1 were decreased in tumors. A similar decrease was previously observed when normal livers from TGFα/c-*myc* mice were compared with liver tumors from the same mice (19). On the other hand, the latter studies found that expression of TR1 was slightly increased in liver tumors relative to surrounding normal livers in TGFα/c-*myc* mice (19). Fig. 1*B* shows immunoblot analyses of mouse TR1 and TR3 enriched from normal wild type and transgenic malignant livers on an ADP-Sepharose column. Proteins isolated from these two sources migrated similarly on SDS-PAGE. TR1 had a molecular mass of ~57 kDa, whereas TR3 migrated as an ~55-kDa protein. Although TR1 is more abundant than TR3 in liver (16), the ratio of these enzymes was approximately the same in wild type and tumor samples (Fig. 2*B*), suggesting that expression of TR3, like that of TR1 (but in contrast to

Alternative First Exon Splicing in Thioredoxin Reductases
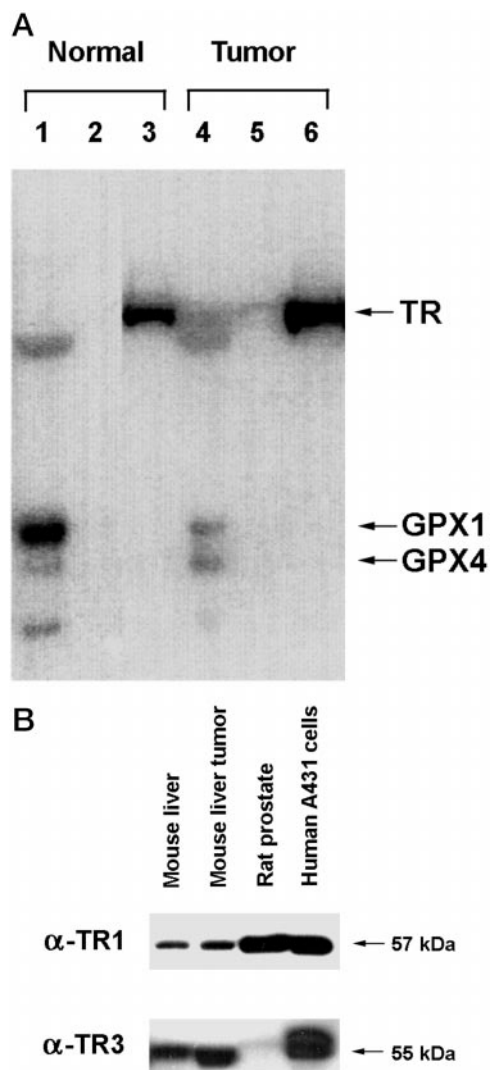
FIG. 1. **Isolation and characterization of mouse liver thioredoxin reductases.** *A*, detection of ^{75}Se by PhosphorImager analysis in fractions from an ADP-Sepharose column. ^{75}Se-Labeled homogenates from wild type livers (*lanes 1–3*) and hepatocarcinomas of TGFα/c-*myc* transgenic mice (*lanes 4–6*) were fractionated on an ADP-Sepharose column. Flow-through (*lanes 1* and *4*), low-salt wash (*lanes 2* and *5*), and high-salt elution (fractions *3* and *6*) fractions were analyzed by SDS-PAGE analysis. The positions of TR (mixture of TR1 and TR3), GPx1 and GPx4 are indicated on the *right*. *B*, immunoblot analyses of mammalian thioredoxin reductases. Wild type liver TR fractions (*A, lane 3*) and liver tumor TR fractions (*A, lane 6*) were probed with antibodies specific for TR1 (*upper panel*). The blot was then stripped and reprobed with antibodies specific for TR3 (*lower panel*). Also analyzed were a homogenous preparation of a rat prostate TR1 obtained by a three-step procedure, employing DEAE-Sepharose, ADP-Sepharose, and phenyl-HPLC columns (shown as Rat prostate, *lane 3*) and a human TR preparation obtained by affinity chromatography of a homogenate from A431 cells on an ADP-Sepharose column (shown as Human A431 cells, *lane 4*). The rat sample did not contain TR3, which had different elution profiles than TR1 from DEAE-Sepharose and phenyl-HPLC columns. The positions of the 57-kDa form of TR1 and the 55-kDa form of TR3 are indicated on the *right*.

GPx1), was unchanged or perhaps somewhat elevated during malignant transformation in TGFα/c-*myc* mice.

In addition to the mouse samples, we analyzed TR1 isolated from rat prostate by a standard three-column procedure (Fig. 1*B, lane 3*), and a TR preparation isolated from a human epidermoid A431 cell line using a single ADP-Sepharose column (Fig. 1*B, lane 4*). Interestingly, although the major form of human TR1 migrated as a 57-kDa band, human TR3 was present as a mixture of 55–57-kDa species.
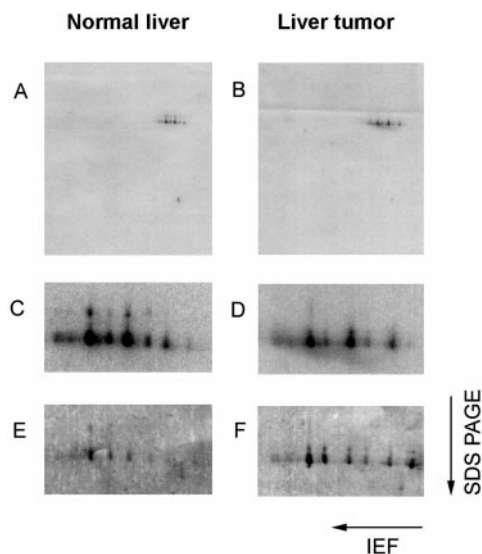
FIG. 2. **Two-dimensional gel electrophoresis of mouse TR preparations.** Wild type liver and TGFα/c-*myc* liver tumor TR preparations were subjected to two-dimensional gel electrophoresis analysis, followed by detection of ^{75}Se by PhosphorImager analysis (*A-D*) and staining of proteins with Ponceau S (*E* and *F*). *Panels A* and *B* show full two-dimensional gels, whereas *panels C-F* show enlarged areas that correspond to ^{75}Se signals on *panels A* and *B*. *Panels A, C,* and *E* show TR1 isolated from wild type livers, and *panels B, D,* and *F*, from liver tumors.

While mouse TR preparations isolated from normal and tumor samples migrated as single species and exhibited similar electrophoretic properties on SDS-PAGE gels (Fig. 1*B*), this electrophoretic technique is often insufficient to resolve minor differences within preparations. Therefore, to further test protein preparations shown in Fig. 1*B, lanes 1* and *2*, we separately analyzed normal and tumor TRs by two-dimensional gel electrophoresis. Comparison of ^{75}Se and protein profiles on two-dimensional gels for normal and tumor samples suggested that all signals shown in Fig. 2 corresponded to TR1. TR3 was not detected on two-dimensional gels because it was present in lower levels than TR1 and exhibited a different isoelectric point.

The two-dimensional gel electrophoresis analysis (Fig. 2) revealed dramatic heterogeneity within TR1 preparations from normal and tumor samples. TR1 bands were separated on two-dimensional gels according to both charge and mass. Nine representative bands from two-dimensional gels for normal and tumor samples (Fig. 2, *E* and *F*) were digested with trypsin. Tryptic digests were analyzed by MALDI time-of-flight mass-spectrometry (MALDI-TOF MS). Experimentally determined peptide masses matched to the peptide masses predicted from the tryptic digestion of a deduced mouse TR1 sequence (see details of mouse TR1 sequences below) and covered >50% of the protein sequence (cysteine-containing and N-terminal peptides were not detected). No post-translational modifications within TR1 that could potentially contribute to different mobilities of TR1 forms on two-dimensional gels were detected. In addition, no significant differences in tryptic peptide maps were found between normal and tumor samples.

In addition to multiple TR1 forms that were resolved by two-dimensional gel electrophoresis (Fig. 2) but migrated as a single 57-kDa band on SDS-PAGE gels (Fig. 1*B*), we detected TR1 forms that significantly differed from the 57-kDa isoforms. We noted that longer exposure of ^{75}Se signals detected with a PhosphorImager and analysis of anti-TR1 immunoblot signals often produced two additional bands, ~67 and ~110 kDa. These bands partially co-purified with the 57-kDa forms and

were present as minor forms in apparently homogeneous enzyme preparations. The 67- and 110-kDa species did not cross-react with anti-TR2 and anti-TR3 antibodies. Migration properties of the 110-kDa minor band corresponded to that of the TR1 homodimer, although the biochemical basis for the possible dimer formation under these conditions is not clear. The possible origin of the 67-kDa band is discussed below.

Heterogeneity within Human Thioredoxin Reductase Preparations—We further tested if the extensive heterogeneity observed within mouse TR1 preparations, occurs in human TR1 preparations. For this purpose, we selected a human T-cell line, JPX9, that was previously used as a source of TR1 (12). To purify human TR1, we initially utilized a previously developed three-step procedure (12). The purified protein was analyzed by electrospray ionization (ESI) mass spectrometry. The recorded ESI-MS spectra showed a broad peak centered at 54,860 Da, that was 230 Da more than the mass predicted from the previously reported human TR1 sequence (24). Reduction and carboxymethylation of the enzyme increased its mass to 55,626 Da, but did not significantly narrow the mass peak. The difference between native and carboxymethylated forms, 762 Da, corresponded to 13.4 alkylated groups. The predicted human TR1 sequence contained 13 cysteines and 1 selenocysteine. Considering that isolated TR1 is often contaminated with a truncated form lacking the last two residues, Sec[498] and Gly[499], the data suggested that the isolated TR1 could be fully alkylated with iodoacetic acid and that cysteines and selenocysteine were not modified in the native enzyme.

We further took advantage of a recent observation that human TR1 could be additionally fractionated on a heparin column (16–18). Indeed, two peaks for TR1 were eluted from the column, which were detected as 280-nm absorbing peaks (Fig. 3). The two peaks could also be detected due the absorbance of a flavin at 450 nm and due to the presence of ^{75}Se in the fractions. Integration of two major TR1 peaks indicated that the second-eluted peak (peak II) had 3.8 times higher selenium content (calculated on the basis of ^{75}Se radioactivity) per mg of protein compared with the first-eluted peak (peak I). The possible reduced selenium content of TR1 in peak I is similar to the previous finding of a HeLa cell TR1 form that had ~0.5 selenium per protein subunit (17). The previously isolated mixture of human T-cell TR1 forms had ~0.74 selenium per protein subunit (12), suggesting that it could be a mixture of TR1 molecules with variable selenium content. Lower levels of selenium may be due to a loss of selenium from TR1 due to hydrolysis in the presence of oxygen or reactive oxygen species, or due to the presence of a truncated form of TR1 lacking C-terminal selenocysteine and glycine residues.

The fractions corresponding to Peak I shown in Fig. 3 were pooled, as were fractions corresponding to Peak II, and the two samples were further analyzed by SDS-PAGE, immunoblot assays, and isoelectric focusing (Fig. 4). Major protein forms in each pool migrated as a 55- and 57-kDa pair of protein bands with approximately similar staining intensity (Fig. 4*A, left panel*). These forms were also detected by immunoblot and PhosphorImager assays (Fig. 4*A, middle* and *right panels*). This observation was in agreement with a previous finding of two closely migrating TR1 forms isolated from human JPX9 cells (12). In addition, the pair of 55- and 57-kDa bands was resolved on gels either run in a nonreducing buffer, or following reduction with dithiothreitol and alkylation with iodoacetic acid, or following denaturation in 6 M guanidine HCl, reduction with dithiothreitol and subsequent carboxymethylation (data not shown).

The 55- and 57-kDa bands were transferred onto a polyvinylidene difluoride membrane, digested with trypsin, and
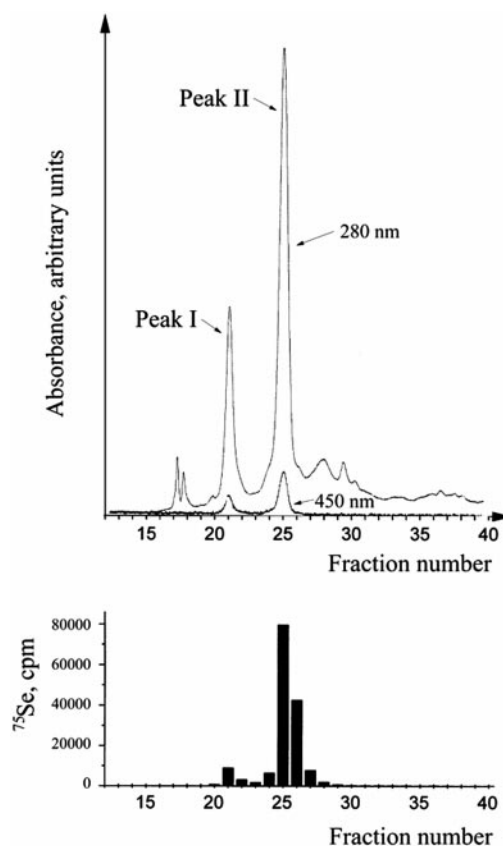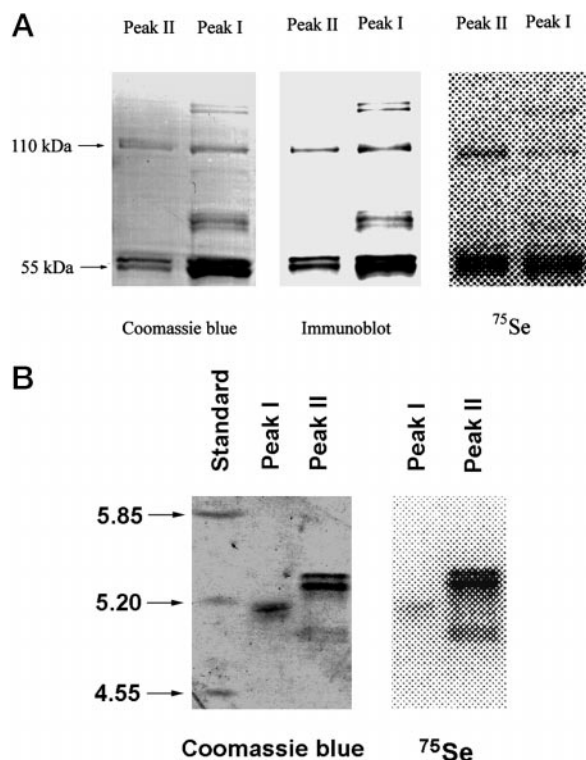

FIG. 3. **Fractionation of human TR1 preparations on a heparin column.** TR1 was first isolated from ^{75}Se-labeled human JPX9 cells using a three-step procedure (12). The enzyme was then further fractionated on a heparin-HPLC column. Proteins eluted were detected by absorbance at 450 (due to the presence of flavin and shown as the smaller signal on the *upper panel*) and 280 nm (shown as the larger signal on the *upper panel*) and by detection of ^{75}Se in fractions from the column using a γ-counter (*lower panel*). For subsequent analyses, fractions corresponding to peak I were pooled, as were those corresponding to peak II, and further analyzed.

masses of tryptic peptides were determined with a MALDI-time of flight MS. Both bands in the doublet produced essentially identical peptide maps and matched with a set of the predicted TR1 tryptic peptides. Even in this instance, we could not detect any Cys-containing peptide, along with the N-terminal and C-terminal peptide. In addition to the 55/57-kDa pair of bands in peaks I and II, a protein form migrating as a 110-kDa band was observed in both TR1 samples (Fig. 4*A*). Like the mouse 110-kDa band, this form corresponded in size to a possible TR1 dimer.

Peaks I and II differed in that a minor ~67-kDa species were present in peak I, but absent in peak II (Fig. 4*A*). This TR1 form was detected as a Coomassie Blue-stained band and as a ^{75}Se-labeled band. It was also reactive in immunoblot assays with anti-TR1 antibodies. Thus, the minor 67-kDa form of TR1 was detected in both mouse and human preparations. In addition, several other minor forms of TR1 were present in peak I of human TR1. Bands with masses higher than 110 kDa could potentially be formed by a dimer formation involving the 67-kDa form.

The protein mixtures present in peaks I and II were further analyzed by tryptic digests followed by determination of peptide masses by MALDI MS. By matching experimentally observed peptide masses with those predicted from an *in silico* tryptic digest of the previously reported human TR1 sequence, we were able to cover over 70% of the human TR1 sequence. Again, no peptide masses were detected that matched Cys-

Alternative First Exon Splicing in Thioredoxin Reductases

A

Peak II Peak I   Peak II Peak I   Peak II Peak I

110 kDa →

55 kDa →

Coomassie blue   Immunoblot ^{75}Se

B

Standard Peak I Peak II   Peak I Peak II

5.85 →

5.20 →

4.55 →

Coomassie blue ^{75}Se

FIG. 4. **Characterization of human TR1 preparations by gel electrophoresis.** *A*, SDS-PAGE analyses. Two TR1 preparations (peaks I and II; see Fig. 3) were subjected to SDS-PAGE analyses followed by detection of proteins by Coomassie Blue staining (*left panel*), immunoblot analyses with antibodies specific for TR1 (*middle panel*), and detection of ^{75}Se by PhosphorImager analyses (*right panel*). For better visualization of protein, immunoblot and ^{75}Se signals, three times more material was loaded on the gel from peak I than from peak II. The positions of the 55- and 110-kDa forms are indicated on the *left*. *B*, isoelectric focusing. Two TR1 preparations (*peaks I and II*) were subjected to isoelectric focusing followed by detection of proteins by Coomassie Blue staining (*left panel*) or detection of ^{75}Se by PhosphorImager analyses (*right panel*). The positions and apparent isoelectric points of three standards are shown on the *left*.

		Exons 1, 2 or 3	Exon 4
MTR1-I	104	tttcaccttccttgttcat	ccgaacaaaaaaaggccaacttcaaaagctgccaacaATGaatggctcc
RTR1-I	57	tttcatcctccttgctcat	ccaaacaaaaaaaggcctacttcgaaagctgtcaacaATGaatgactct
MTR1-II	203	ccatggtccagccctgaag	ccgaacaaaaaaaggccaacttcaaaagctgccaacaATGaatggctcc
RTR1-II	25	ccatggtccagccctgaag	ccaaacaaaaaaaggcctacttcgaaagctgtcaacaATGaatgactct
MTR1-III		aaatacgcaatctgagctg	ccgaacaaaaaaaggccaacttcaaaagctgccaacaATGaatggctcc
RTR1-III		aaatacacgacctgggctg	ccaaacaaaaaaaggcctacttcgaaagctgtcaacaATGaatgactct
RTR1 gene	4530	ttatgttgttttcctgcag	ccaaacaaaaaaaggcctacttcgaaagctgtcaacaATGaatgactct

FIG. 5. **Nucleotide sequence comparisons of TR1 forms obtained by alternative first exon splicing in mice and rats.** Each of the three forms was represented by mouse and rat sequences. The three forms had distinct 5′ sequences (*exons 1, 2,* or *3*), but shared downstream sequences (*exon 4*). Shown in this figure are: MTR1-I, first form of mouse TR1 (accession number AB027565, dbNR cDNA sequence); MTR1-II, second form of mouse TR1 (accession number AI956288, dbEST sequence); MTR1-III, third form of mouse TR1 (this work); RTR1-I, first form of rat TR1 (accession number AF220761, dbNR cDNA sequence); RTR1-II, second form of rat TR1 (accession number AF108213, dbNR cDNA sequence); RTR1-III, third form of rat TR1 (accession number AF189711, dbNR genomic sequence); and RTR1 gene, partial sequence of the rat TR1 gene (accession number AF189711, dbNR genomic sequence). ATG codons that correspond to the previously predicted initiation site within mammalian TR1 sequences are shown in *uppercase*. Intronic sequence is boxed. The *vertical line* indicates sites for junction of exons 1, 2, or 3 to exon 4. *Numbers* on the *left* correspond to nucleotide numbers for GenBank™ sequences shown in the figure.

containing, N-terminal and C-terminal peptides. Spectra obtained from peak I and peak II were virtually identical. The only differences detected were an ion signal at 2110 Da present only in peak I and signals at 1446 and 1430 Da present only in peak II. These peptides could not be assigned in the human TR1 sequence.

Despite the close similarity observed by SDS-PAGE and mass spectrometry analyses between the various TR1 forms present in peaks I and II (Fig. 4*A*), these proteins had different migration properties when analyzed by isoelectric focusing (Fig. 4*B*). Each form was represented by several protein bands (Fig. 4*B*). Overall, the data indicated the presence of multiple forms of human TR1 that differed in molecular masses and isoelectric points.

Alternative First Exon Splicing Results in the Formation of Three Distinct mRNA Isoforms of Mouse and Rat TR1—Having determined no post-translational modifications, we tested whether observed heterogeneity within human and mouse TR1 preparations could be explained by genetic variations within TR1 sequences. In particular, the occurrence of the 67-kDa form of TR1, which was ~10 kDa larger than the protein deduced from known mammalian TR1 cDNAs, could not be easily explained without invoking genetic mechanisms. During the time of our analysis, no mouse TR1 sequences were available in GenBank™. Therefore, we obtained a cDNA sequence of mouse TR1 by sequencing multiple EST clones. Surprisingly, the final 3626-nucleotide cDNA sequence encoded a protein of

613 residues that had a predicted mass of 67.1 kDa. The deduced polypeptide contained the C-terminal penultimate selenocysteine residue encoded by a TGA codon and all sequence features found in other animal TR sequences (N-terminal disulfide active center, NADPH- and FAD-binding domains and a dimer-interface domain). The predicted protein differed from the previously reported 499-amino acid sequences for mammalian TR1s (24, 25) in that the mouse protein had 114 additional N-terminal residues. The new N-terminal sequence had no homology to coding regions of other proteins when analyzed using BLAST programs against nonredundant (NR) and EST data bases, except that it exhibited >70% identity with sequences deduced from a rat genomic clone that contained a partial sequence of the TR1 gene (accession number AF189711).

A second mouse TR1 sequence, which encoded a 499-amino acid protein, has recently appeared in GenBank™ (accession number AB027565). Comparison of two mouse TR1 cDNA sequences revealed identity in >3 kilobases that spanned most of the coding region and the entire 3′-untranslated region. These sequences, however, had no homology in 5′-end sequences (Fig. 5). Subsequent BLAST analyses of mouse dbEST revealed a mouse EST sequence (accession number AI956288) corresponding to a third TR1 form that had an additional distinct version of the 5′-end sequence, but was identical with the two full-size cDNA sequences in the downstream region (Fig. 5). The use of three independent 5′ variants deviating from each other at the same place within the nucleotide sequence was reminiscent of the alternative use of three exons; that is, different 5′ sequences corresponded to alternative first exons, while common sequences corresponded to common downstream exons.

This proposition was consistent with the BLAST analysis of rat NR and EST data bases using sequences for three forms of mouse TR1 mRNA. It revealed three potential forms of rat TR1 mRNA that corresponded to the three mouse mRNA forms (Fig. 5). Moreover, the availability of the partial sequence for the rat TR1 gene allowed us to predict partial features of an exon-intron structure within this region (Fig. 6). The first exon within the rat genomic sequence corresponded to the 5′ end of our mouse TR1 cDNA sequence, whereas the second exon that was separated from the first exon by an ~1.5-kilobase long
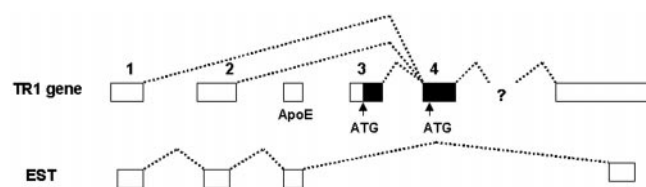
FIG. 6. **Predicted structural organization of mouse and rat TR1 genes.** Upper portion of the figure shows organization of the TR1 gene in mice and rats. Three alternative forms of TR1 mRNA are obtained from a single TR1 gene by initiating transcription at exons 1, 2, or 3 (indicated by *numbers* above exon boxes), followed by alternative splicing to link a used exon to exon 4. The downstream organization of the gene is not known (shown as *question mark*). ATG codons indicate alternative translation initiation sites. *Filled boxes* indicate translated sequences. *Open boxes* correspond to untranslated regions. Lower portion of the figure shows organization of several ESTs (accession numbers AI526517, AI527732, AI226627, AI787452, AI314145, and AI315024) that were used to determine the order of exons in the TR1 gene. These ESTs contained sequences that were identical with partial sequences of exon 1, exon 2, and the last exon of the TR1 gene. In addition, ESTs contained an internal stretch of sequences identical with internal sequences of exon 4 of apolipoprotein E gene (shown as ApoE in the upper portion of the figure).

intron, corresponded to the first common exon within the three forms.

The three TR1 forms, TR1-I, TR1-II, and TRI-III (Fig. 6), were designated according to order of exons within genomic sequences, which was derived from the following observations. The first exon of the TR1-III sequence was present in the rat genomic clone that also contained the downstream sequences common for three TR1 forms, whereas the first exons of the TR1-I and TR1-II sequences were not present in the rat genomic clone sequence. Thus, 5′ exons of TR1-I and TR1-II were upstream of the 5′ exon of TR1-III. We also found several EST sequences (accession numbers AI526517, AI527732, AI226627, AI787452, AI314145, and AI315024) that contained partial sequences for first exons of TR1-I and TR1-II as well as downstream sequences that were common for the three forms (Fig. 6). Within these ESTs, 5′ sequences of TR1-I preceded 5′ sequences of TR1-II. Thus, within the genomic sequences, the 5′ exon of TR1-I should be first, the 5′ exon of TR1-II, second, and the 5′ exon of TR1-III, third, followed by a fourth exon that had sequences common for the three TR1 forms.

Interestingly, ESTs that contained 5′ sequences for TR1-I and TR-II had an additional internal stretch of 176 nucleotides, which was 100% identical to internal sequences of exon 4 of a mouse apolipoprotein E (ApoE) gene. It should be noted that known TR1 (chromosome 10) and ApoE (chromosome 7) genes in mice are located on different chromosomes. If ESTs containing TR1 and ApoE sequences were formed by alternative splicing, then one possible explanation for their formation is that mice may have an additional ApoE gene or a pseudogene located within the TR1 gene. Alternatively, ESTs containing a 176-nucleotide stretch could be formed by possible novel genetic mechanisms (such as "reverse splicing"), which would allow insertion of a DNA (or mRNA) sequence within another DNA (or mRNA) sequence.

Alternative Use of First Exons within TR3 Genes—The observation of alternative mRNA forms of TR1 in rats and mice prompted us to test whether this mechanism is used in genes for other TRs. Indeed, computer search analysis of NR and EST data bases revealed three alternative human TR3 transcripts (TR3-I, TR3-II, and TR3-III) that differed in their 5′ sequences (Fig. 7) and were formed by alternative first exon splicing (Fig. 8). TR3-I (accession numbers AF171054, AF044212, AF106697, and AB019694) was a previously reported nucleus-encoded mitochondrial form of TR3 (5–10). The TR3-II transcript (accession number AF166127) was a previously identified isoform of


FIG. 7. **Sequence comparisons of TR3 forms obtained by alternative first exon splicing in mice, rats, and humans.** *A*, nucleotide sequence comparisons of three alternative TR3 cDNA forms. The three forms utilize alternative first exons (*exons 1, 2, or 3*), followed by the common exon (*exon 4*). Exon-intron splicing sites are shown by interruptions in *horizontal lines*. Exonic sequences are shown in *uppercase*, and intronic sequences, in *lowercase*. *Numbers* on the *left* and *right* indicate nucleotide numbers within GenBank™ genomic sequences that were used to assemble the figure. *Numbers within* sequences indicate numbers of intronic nucleotides present within sequences shown in the figure. ATG codons that are predicted to initiate translation of TR3-III mRNAs are shown in *bold*. These are characterized by favorable Kozak consensus sequences for phasing mRNA for initiation of translation. The occurrence of exons 2 and 3 in human sequences is indicated by the analysis of dbNR. The occurrence of exon 3 in mouse and rat sequences is predicted in this study based on the analysis of mouse and rat genomic sequences with an exon-searching program. Sequences shown are from the following dbNR genomic sequences: HTR3-I, first form of human TR3 (accession number AC000090), MTR3-I, first form of mouse TR3 (accession number AC003066), RTR3-I, first form of rat TR3 (accession number RN5CATOMT), HTR3-II, second form of human TR3 (accession number AC000090), HTR3-III, third form of human TR3 (accession number AC000090); MTR3-III, third form of mouse TR3 (accession number AC003066); RTR3-III, third form of rat TR3 (accession number RN5CATOMT). *B*, amino acid sequence comparisons of TR3-I and TR3-III. Same sequences were used here as in Fig. 7A. Exon-intron junctions (indicated by interruptions within *horizontal lines*) were predicted with an exon finding program and by matching cDNA and genomic sequences.

human TR3 mRNA, SelZf2 (26). This transcript appeared to be inhibitory for TR3 expression since it contained an initiator ATG codon, followed by an in-frame stop signal, in a different frame with established TR3 sequences. The TR3-III transcript (accession number AB019695) encoded a protein that lacked a mitochondrial signal but instead contained a 5-amino acid extension. The lack of signal peptides in TR3-III suggested that the protein could reside in the cytosol.

The human TR3 gene, located on chromosome 22 (accession number AC000090), was previously sequenced by the Human Genome Project as evidenced by the BLAST analysis of dbNR. Organization of the human TR3 gene and its upstream region are shown in Fig. 8. Comparison of cDNA and genomic sequences indicated that alternative TR3-I, TR3-II, and TR3-III transcripts were formed due to alternative use of three 5′ exons within the gene. We also analyzed partial sequences of the mouse TR3 gene (accession number AC003066, clone tbx1, strain 129X1/SvJ ES, from cell line RW4, located on chromosome 16) that were generated by the Mouse Genome Project and partial rat TR3 genomic sequences that were found in the genomic clone containing an upstream region of the COMT gene. Analyses of these sequences with an exon finding pro-
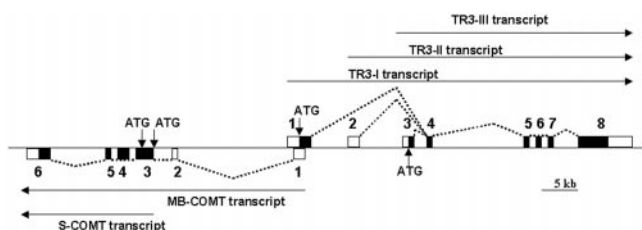
FIG. 8. **Structural organization of human TR3 and COMT genes.** TR3 and COMT genes are located on complementary DNA strands and overlap in their first exons such that transcription within the membrane-bound form (MB-COMT) of the COMT gene is initiated within the coding region of the mitochondrial (TR3-I) form of the TR3 gene. However, transcription start sites in the TR3-III gene and a soluble form (*S-COMT*) of the COMT gene are separated by ~30 kilobases. Alternative first exon splicing is used in the TR3 gene. TR3-I mRNA is composed of 6 exons (exons 1 and 4–8); TR3-II mRNA, 6 exons (exons 2 and 4–8); TR3-III mRNA, 6 exons (exons 3–8); MB-COMT mRNA, 6 exons (exons 1–6); and S-COMT mRNA, 4 exons (exons 3–6). Translation start sites within TR3 and COMT genes are indicated by ATG codons. Initiator ATG codon for TR3-I mRNA is located within exon 1, and for TR3-III mRNA, within exon 2. Translation start site for TR3-II is located within exon 2, but followed by an in-frame stop signal (not shown). The translation initiation site in the MB-COMT mRNA is the first ATG within exon 3, and in the S-COMT mRNA, the second ATG within exon 3. *Filled boxes* indicate translated sequences. *Open boxes* correspond to untranslated regions.

gram revealed the presence of a predicted conserved exon that could generate TR3-III forms of mouse and rat TR3 (Fig. 7). Thus, the use of alternative first exon splicing to form multiple TR3 forms appeared to be conserved in humans, mice, and rats. However, no ESTs that corresponded to mouse and rat TR3-III were detected.

We have previously noted that the human TR3 gene partially overlapped with the gene for COMT (10). In the present study, we performed detailed computer analysis of human TR3 and COMT genes and analyzed whether this structural organization of these genes is conserved in other animals. We found that the first exon of the human TR3 gene overlapped with the first exon of the gene for membrane-bound (MB)-COMT (Fig. 8). The mTR3 and MB-COMT genes were located on different DNA strands on a chromosome 22q11.2 band. Translation of MB-COMT mRNA resulted in the 30-kDa protein containing an N-terminal transmembrane domain (27). Interestingly, the COMT gene, like the human TR3 gene, had an additional transcription initiation site. The use of this site resulted in a transcript that lacked the first two exons and translated into a shorter 26-kDa soluble catechol-*O*-methyltransferase (S-COMT) (27). Human DNA sequences containing exon 1 of the TR3-I gene and exon 1 of the MB-COMT gene were well separated from other exons within these genes. For example, transcription start sites for S-COMT and TR3-III were separated by ~30 kilobases (Fig. 8).

Further analysis of mouse and rat TR3 genes revealed that exons encoding a mitochondrial signal overlapped with the first exons of mouse and rat MB-COMT genes. Conservation of structural organization of TR3 and COMT genes in humans, mice, and rats suggested that certain TR3 and COMT forms could potentially exhibit parallel or contrasting regulation of expression.

Alternative Use of First Exons in the Drosophila TR Gene—In addition to the finding of alternative first exons within mammalian TR genes, we detected a *Drosophila* gene for TR that produced two alternative transcripts (Fig. 9). Like TR3 forms, these transcripts encoded proteins that differed in their N-terminal regions. The previously reported *Drosophila* TR sequence (accession number U81995) corresponded to a putative cytosolic form of this enzyme, while the additional form of the protein was evident from the BLAST analysis of dbEST and
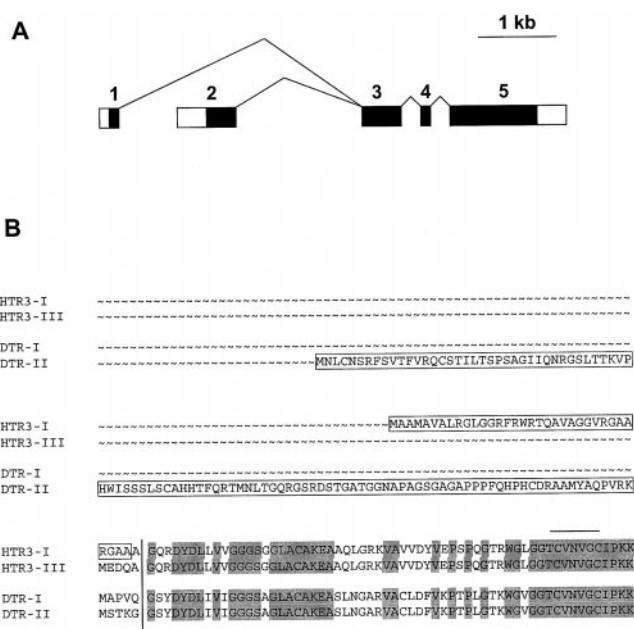
FIG. 9. **Alternative forms of *Drosophila* TR.** *A*, structural organization of the *Drosophila* TR gene. Each *numbered box* represents an exon within the gene. *Open boxes* show untranslated regions, and *filled boxes*, coding regions. There are two alternative forms of *Drosophila* TR mRNA that are encoded by either exons 1 and 3–5 (DTR-I, accession number U81995), or exons 2–5 (DTR-II; accession number AA803764 and AA820592). *B*, amino acid sequences of N-terminal regions of two alternative *Drosophila* TR sequences. Human TR3-I and TR3-III, which deviate from each other at the same site within the intron-exon structure, are shown for comparison. *Boxed* residues represent predicted mitochondrial signal peptides. The *vertical line* represents exon-intron junctions. Identical residues within four sequences are *highlighted*. The *horizontal line* over the sequences shows the location of the disulfide active center.

was represented by several ESTs (*e.g.* accession numbers AA803764 and AA820592 and 6 other ESTs). This second form of the *Drosophila* TR contained a predicted mitochondrial signal peptide. Thus, it is likely that a single *Drosophila* TR gene encodes two proteins, mitochondrial and cytosolic. Interestingly, although the order of predicted mitochondrial and cytosolic exons was different, the location of the splicing site that separated variable and common sequences was conserved between mammalian TR3 and *Drosophila* TR genes (Fig. 9*B*).

DISCUSSION

We report in the present study that extensive heterogeneity exists among animal TRs and that splicing of first exons of TR genes occurs as a general genetic mechanism for producing multiple mRNA isoforms. The data suggest that this evolutionary conserved genetic mechanism contributes to heterogeneity that is observed among animal TRs.

The fact that human TR1 isolated from HeLa cells occurs in at least two distinct forms has been established previously (16–18). The two forms could be separated by affinity chromatography on a heparin column. The first form was not retained on a heparin column, exhibited full catalytic activity and selenium content and showed reactivity with anti-rat liver TR1 antibodies. This form could be converted into the high-affinity TR1 form upon reduction. An additional TR1 form was also isolated that could bind the heparin column without prior reduction. This form contained ~0.5 selenium per subunit and had reduced catalytic activities and reactivity with anti-rat liver TR1 antibodies.

Our present study indicates that the number of TR1 forms is much larger than previously thought and that these forms differ in electrophoretic mobility on SDS-PAGE and isoelectro-

focusing gels. In particular, minor 67-kDa isoforms of TR1 were detected in our study that migrated significantly slower on SDS-PAGE gels than would be predicted from previously reported gene sequences. To characterize various mouse TR1 forms, we used affinity chromatography on ADP-Sepharose. Interestingly, this simple technique was sufficient to enrich TR1 to an extent that it could be directly analyzed on two-dimensional gels and visualized by protein staining. Since multiple forms of TR1 were visualized after only a single isolation step, this procedure may provide a basis for future high-throughput protein microchemistry analyses of TRs isolated from multiple sources or under various conditions.

To define the basis for heterogeneity within human and mouse enzyme preparations, we initially used protein microchemistry techniques and established that detected tryptic peptides did not differ between various enzyme isoforms that had different electrophoretic mobility on polyacrylamide gels or were isolated from normal or malignant cells. It remains to be determined what post-translational modifications, if any, are involved in the formation of 55–57-kDa TR1 forms in humans and mice.

To further characterize a mechanism responsible for the formation of multiple TR1 forms and, in particular, for the occurrence of 67-kDa TR1 species, we turned our attention to possible genetic mechanisms. Since no mouse TR1 sequences were available in sequence data bases, we initially determined the mouse TR1 cDNA sequence. Interestingly, this cDNA encoded a protein of 67 kDa that was formed from a coding region starting with an ATG codon (in a favorable Kozak consensus sequence for phasing the message for translation) upstream of the previously predicted translation start site. The predicted extended N-terminal domain had no homology to known protein sequences, and at present its function is not known.

Recently, several new mammalian TR1 cDNA sequences, including one for mouse TR1 (28), were deposited into Gen-Bank™. Examination of NR and EST sequences and their comparison to the mouse TR1 cDNA sequence that was determined in the present study, revealed three forms of mouse and rat TR1 cDNAs that had unrelated 5′ sequences, but common downstream sequences. We also observed three human TR1 forms (BE618239, AU077310, and previously known TR1 sequences) obtained by alternative exon splicing. The location of an alternative splicing site was conserved among mouse, rat, and human TR1 genes.

Alternative first exon splicing that was found to be used to synthesize alternative mRNA forms of mouse and rat TR1 mRNA is a previously recognized genetic phenomenon (29). It is used to accommodate requirements for elevated expression of a protein in a tissue-specific manner and to synthesize protein species that differ in their intracellular location (*e.g.* alternative forms may contain or lack an organelle-targeting signal peptide or a trans-membrane domain). In addition, alternative first exon splicing may be used as an on/off switch, which functions by alternative expression of protein-expressing and protein-suppressing mRNA forms. In this case, the "off" form would contain additional upstream initiation sites followed by stop signals that would suppress protein expression, whereas the "on" form would produce a functional protein.

Well characterized examples of alternative first exon splicing include genes of enzymes that are involved in "liver-associated" xenobiotic metabolism and detoxification. The human microsomal glutathione *S*-transferase utilizes four alternative first exons, two of which appear to be functional and result in mRNA sequences differing in the 5′-untranslated region, and two non-functional forms as they contain additional upstream out of frame initiation signals (30). These four mRNA forms were predicted to be generated from a common promoter. The rat γ-glutamyltransferase gene also has four alternative first exons but utilizes four alternative promoters to form mRNA species differing in the 5′-untranslated region but encoding identical proteins (31). Additional examples of alternative first exon splicing include family 19 of the cytochrome P450 gene superfamily (32) and the UDP-glucoronosyltransferase gene (33), which contain numerous first exons but a common splice junction located upstream of the translation start site.

One interesting observation made in the present study is that several mouse ESTs contained apolipoprotein E sequences within the TR1 sequences. Since all these ESTs originate from the same cDNA library (Sugano mouse kidney mkia), additional sequences from other sources may be required to confirm the observed puzzling location of the ApoE sequences. If confirmed, the finding that an ApoE gene is located within the mouse TR1 gene may have important biomedical implications. Previous molecular genetic studies identified three genes (presenilin 1, presenilin 2, and β-amyloid precursor protein) associated with early onset of Alzheimer's disease (AD), and one gene (ApoE) associated with late onset of AD (34). An additional AD susceptibility locus has been mapped to a broad region of chromosome 12, but the gene responsible for a defect has not been identified. Whereas the human ApoE gene resides on chromosome 19, the TR1 gene is located on human chromosome 12. If a mouse TR1 gene indeed contains an additional ApoE gene and this gene organization is conserved in humans, then a new ApoE gene may provide an additional susceptibility marker for AD. Alternatively, the ApoE sequences located within the mouse TR1 gene may be a part of an ApoE pseudogene, or the internal ApoE sequences could have been incorporated into TR1 sequences by an unknown genetic mechanism. To confirm the predicted organization of mouse and rat TR1 genes and to determine the actual mechanism involved in linking TR1 and ApoE sequences, we have to wait until actual sequences of TR1 genes are available.

Having determined the use of alternative first exon splicing in regulation of expression of mouse and rat TR1 mRNAs, we tested whether this mechanism is used to express multiple forms of other TRs. Indeed, two unrelated 5′-end sequences, followed by common downstream sequences were evident from the analysis of two human TR2 cDNA sequences (EST sequence, accession number AA460989, and a cDNA sequence, accession number AF133519). However, the lack of full-size cDNAs and genomic sequences for mammalian TR2 did not allow us to evaluate the significance of this finding.

The analysis of mammalian TR3 genes was more fruitful and revealed a remarkable genetic complexity within genomic segments that contained TR3 genes. Like mouse and rat TR1 genes, the human TR3 gene contained three alternative first exons. However, the previously defined translation initiation site was located upstream of the first common exon and thus the use of alternative first exons resulted in different N-terminal sequences of the protein. The use of exon 1 resulted in the formation of a mitochondrial form of the enzyme, TR1-I (exon 1 encoded a mitochondrial signal peptide). The use of exon 2 instead of exon 1 generated an mRNA form (TR3-II) that contained an upstream out of frame initiation site followed by a termination signal. This form could potentially be used as an off switch. If exon 3 was used in place of either exon 1 or exon 2, the N-terminal sequence of TR3 was extended by only 5 residues. The lack of signal sequences within TR3-III suggested that this protein could be located in the cytosol.

Such a complex organization of TR3 genes was even more complicated by the fact that exon 1 of human, mouse, and rat TR3 genes overlapped with exon 1 of the MB-COMT gene

located on a complementary DNA strand. It has previously been established that the COMT gene gives rise to two alternative protein forms, a membrane-bound and a soluble form (27). Only the MB-COMT mRNA had common sequences with TR3 mRNA, and only TR3-I mRNA (mitochondrial form) overlapped with MB-COMT mRNA. Interestingly, the COMT knockout mice have been previously generated and found to exhibit sexually dimorphic changes in catecholamine levels and behavior (35). No sufficient experimental details were reported (35) to evaluate whether knockouts could have affected expression of some of the TR3 forms. It is also not known whether TR3 could be involved in psychiatric disorders and symptoms, including the psychopathology associated with the 22q11 microdeletion, the area of the human chromosome 22, where the COMT and TR3 genes are located.

Availability of the completely sequenced *Drosophila* genome and a large number of EST sequences allowed us to test if alternative first exon splicing is also used in *Drosophila*. We identified two alternative exons within the *Drosophila* TR gene that generated predicted mitochondrial and cytosolic enzymes. Interestingly, the site for junction of alternative first exons and a common downstream exon was conserved between mammalian TR3 and *Drosophila* TR genes, suggesting a close evolutionary relation between these genes. In addition, homology and phylogenetic analyses (data not shown) indicated slightly higher evolutionary linkage between *Drosophila* TR and mammalian TR3 genes than between mammalian TR1 and TR3 genes.

In conclusion, we identified alternative exon splicing as a general mechanism to express multiple mRNA forms of animal TRs. Such mRNA forms encoded proteins that have common or different N-terminal sequences and that were responsible, at least in part, for observed heterogeneity within animal TR preparations. The use of alternative first exon splicing has not been described previously for any known selenoprotein. Further studies are required to determine the functional role of alternative first exon splicing in regulation of expression and function of animal thioredoxin reductases.

Addendum—A recent paper by Rundlof *et al.* (36) also reported identification of three variants of rodent TR1 mRNA.

REFERENCES

1. Sies, H. (1999) *Free Radic. Biol. Med.* **27,** 916–921
2. Holmgren, A. (1989) *J. Biol. Chem.* **264,** 13963–13966
3. Halliwell, B. (1999) *Free Radic. Res.* **31,** 261–272
4. Matsui, M., Oshima, M., Oshima, H., Takaku, K., Maruyama, T., Yodoi, J., and Taketo, M. M. (1986) *Dev. Biol.* **178,** 179–185
5. Gasdaska, P. Y., Berggren, M. M., Berry, M. J., and Powis, G. (1999) *FEBS Lett.* **442,** 105–111
6. Lee, S. R., Kim, J. R., Kwon, K. S., Yoon, H. W., Levine, R. L., Ginsburg, A., and Rhee, S. G. (1999) *J. Biol. Chem.* **274,** 4722–4734
7. Miranda-Vizuete, A., Damdimopoulos, A. E., Pedrajas, J. R., Gustafsson, J. A., and Spyrou, G. (1999) *Eur. J. Biochem.* **261,** 405–412
8. Watabe, S., Makino, Y., Ogawa, K., Hiroi, T., Yamamoto, Y., and Takahashi, S. Y. (1999) *Eur. J. Biochem.* **264,** 74–84
9. Miranda-Vizuete, A., Damdimopoulos, A. E., and Spyrou, G. (1999) *Biochim. Biophys. Acta* **1447,** 113–118
10. Sun, Q.-A., Wu, Y., Zappacosta, F., Jeang, K.-T., Lee, B. J., Hatfield, D. L., and Gladyshev, V. N. (1999) *J. Biol. Chem.* **274,** 24522–24530
11. Tamura, T., and Stadtman, T. C. (1996) *Proc. Natl. Acad. Sci. U. S. A.* **93,** 1006–1011
12. Gladyshev, V. N., Jeang, K.-T., and Stadtman, T. C. (1996) *Proc. Natl. Acad. Sci. U. S. A.* **93,** 6146–6151
13. Fujiwara, N., Fujii, T., Fujii, J., and Taniguchi, N. (1999) *Biochem. J.* **340,** 439–444
14. Lee, S. R., Bar-Noy, S., Kwon, J., Levine, R. L., Stadtman, T. C., and Rhee, S. G. (2000) *Proc. Natl. Acad. Sci. U. S. A.* **97,** 2521–2526
15. Gasdaska, J. R., Harney, J. W., Gasdaska, P. Y., Powis, G., and Berry, M. J. (1999) *J. Biol. Chem.* **274,** 25379–25385
16. Liu, S. Y., and Stadtman, T. C. (1997) *Proc. Natl. Acad. Sci. U. S. A.* **94,** 6138–6141
17. Gorlatov, S. N., and Stadtman, T. C. (1998) *Proc. Natl. Acad. Sci. U. S. A.* **95,** 8520–8525
18. Gorlatov, S. N., and Stadtman, T. C. (1999) *Arch. Biochem. Biophys.* **369,** 133–142
19. Gladyshev, V. N., Factor, V. M., Housseau, F., and Hatfield, D. L. (1998) *Biochem. Biophys. Res. Commun.* **251,** 488–493
20. Appella, E., Arnott, D., Sakaguchi, K., and Wirth, P. J. (2000) *EXS (Exper. Suppl.)* **88,** 1–27
21. Sutton, C. W., Pemberton, K. S., Cottrell, J. S., Corbett, J. M., Wheeler, C. H., Dunn, M. J., and Pappin, D. J. (1995) *Electrophoresis* **16,** 308–316
22. Zappacosta, F., Borrego, F., Brooks, A. G., Parker, K. C., and Coligan, J. E. (1997) *Proc. Natl. Acad. Sci. U. S. A.* **94,** 6313–6318
23. Altschul, S. F., Madden, T. L., Schäffer, A. A., Zhang, J., Zhang, Z., Miller, W., and Lipman, D. J. (1997) *Nucleic Acids Res.* **25,** 3389–3402
24. Gasdaska, P. Y., Gasdaska, J. R., Cochran, S., and Powis, G. (1995) *FEBS Lett.* **373,** 5–9
25. Zhong, L., Arner, E. S., Ljung, J., Aslund, F., and Holmgren, A. (1998) *J. Biol. Chem.* **273,** 8581–8591
26. Lescure, A., Gautheret, D., Carbon, P., and Krol, A. (1999) *J. Biol. Chem.* **274,** 38147–38154
27. Tenhunen, J., Salminen, M., Lundstrom, K., Kiviluoto, T., Savolainen, R., and Ulmanen, I. (1994) *Eur. J. Biochem.* **223,** 1049–1059
28. Kawai, H., Ota, T., Suzuki, F., and Tatsuka, M. (2000) *Gene* **242,** 321–330
29. Breitbart, R. E., Andreadis, A., and Nadal-Ginard, B. (1987) *Annu. Rev. Biochem.* **56,** 467–495
30. Kelner, M. J., Bagnell, R. D., Montoya, M. A., Estes, L. A., Forsberg, L., and Morgenstern, R. (2000) *J. Biol. Chem.* **275,** 13000–13006
31. Okamoto, T., Darbouy, M., Brouillet, A., Lahuna, O., Chobert, M. N., and Laperche, Y. (1994) *Biochemistry* **33,** 11536–11543
32. Simpson, E. R., Michael, M. D., Agarwal, V. R., Hinshelwood, M. M., Bulun, S. E., and Zhao, Y. (1997) *FASEB J.* **11,** 29–36
33. Strassburg, C. P., Oldhafer, K., Manns, M. P., and Tukey, R. H. (1997) *Mol. Pharmacol.* **52,** 212–220
34. St. George-Hyslop, P. H. (1999) *Semin. Neurol.* **19,** 371–383
35. Gogos, J. A., Morgan, M., Luine, V., Santha, M., Ogawa, S., Pfaff, D., and Karayiorgou, M. (1998) *Proc. Natl. Acad. Sci. U. S. A.* **95,** 9991–9996
36. Rundlof, A. K., Carlsten, M., Giacobini, M. M., and Arner, E. S. (2000) *Biochem. J.* **347,** 661–668